A new simple equation for the prediction of filter expansion during backwashing

Elif Soyer and Omer Akgiray

ABSTRACT

Fluidization experiments have been carried out with glass spheres, plastic spheres and several sieved fractions of silica sand, garnet sand, perlite and crushed glass. The effect of particle shape on expansion behavior is investigated. Sphericity as determined using the Ergun equation and fixed-bed head loss data is employed to quantify the shape effect. It is found that the influence of particle shape depends on the Reynolds number based on backwash velocity. A new equation that accounts for particle shape is proposed. For the materials studied, the proposed equation gives excellent agreement with both the spherical and the non-spherical particle data.

Key words | backwash, filter media, fluidization, particle shape, sphericity, water treatment

Elif Soyer (corresponding author)
Department of Environmental Engineering,
Istanbul Technical University,
Maslak-Istanbul,
Turkey
Tel.: +90 212 285 6785
Fax: +90 212 285 3781
E-mail: *esoyer@ins.itu.edu.tr*

Omer Akgiray
Department of Environmental Engineering,
Marmara University,
Goztepe-Istanbul,
Turkey

INTRODUCTION AND THEORY

Liquid–solid fluidization has a number of applications in engineering (Epstein 2003b). The expansion of granular filter media during backwashing is of particular interest (Droste 1997; AWWA 1999; Akkoyunlu 2003). It is important to have an understanding of fluidization principles and an ability to predict bed expansion as a function of liquid velocity to design such systems properly. More often than not, the media involved are not spherical and it is necessary to have an expansion model that can be applied to beds of non-spherical particles.

Numerous equations have been proposed to predict the expansion of liquid fluidized beds of spheres. Reviews and listings of such equations can be found in Garside & Al-Dibouni (1977), Couderc (1985), Hartman *et al.* (1989), Di Felice (1995) and Epstein (2003a). An evaluation of these equations has recently been presented by Akgiray & Soyer (2006). Very few general equations exist, however, for non-spherical media (Cleasby & Fan 1981; Dharmarajah & Cleasby 1986; Akgiray & Saatçi, 2001; Akkoyunlu 2003; Akgiray *et al.* 2004). Furthermore, the accuracies of the expansion models for non-spherical media have not been evaluated in a satisfactory manner to date.

Akgiray & Soyer (2006) noted that, while most expansion models are strictly restricted to spheres, a correlation method explained by Richardson & Meikle (1961) may be generalized to handle non-spherical media. In this approach, a dimensionless friction factor f is plotted against a modified Reynolds number Re_1. The friction factor is defined as follows:

$$f = \frac{R}{\rho\left(\frac{V}{\varepsilon}\right)^2} \tag{1}$$

where R = force per unit area of grains, ρ = density of the fluid, ε = porosity of the bed and V = fluid velocity based on the empty cross section of the bed. The porosity ε for the fluidized bed is calculated by the relation $L(1 - \varepsilon) = L_0(1 - \varepsilon_0)$, where L = depth of the fluidized bed, L_0 = depth of the fixed bed and ε_0 = fixed-bed porosity. Equation (1) holds for both fixed and fluidized beds. For a fluidized bed under steady state conditions, the upward frictional force on the particles is balanced by the effective gravitational force. The net gravitational force is the weight of the particles less the upward force attributable

to the buoyancy of the suspension. Therefore, Equation (1) takes the following form for fluidized beds under steady state conditions:

$$f = \frac{\varepsilon^3(\rho_p - \rho)g}{\rho\left(\frac{S_p}{V_p}\right)V^2} = \frac{\varepsilon^3(\rho_p - \rho)g\psi d_{eq}}{6\rho V^2} \quad (2)$$

Here, $S_p/V_p = 6/(\psi d_{eq})$ is the specific surface of the grains, S_P = particle surface area, V_P = particle volume, ρ_p = particle density, d_{eq} = equivalent diameter defined as the diameter of the sphere with the same volume as the particle, ψ = sphericity defined as the surface area of the equivalent volume sphere divided by the actual surface area of the particle and g = gravitational acceleration. The definition of Re_1 uses interstitial velocity V/ε for the characteristic velocity and the mean hydraulic radius $\varepsilon/((S_p/V_p)(1 - \varepsilon))$ for the characteristic linear dimension (Blake 1922):

$$Re_1 = \frac{V}{\varepsilon} \frac{\varepsilon}{(S_p/V_p)(1 - \varepsilon)} \frac{\rho}{\mu} = \frac{\psi d_{eq}\rho V}{6\mu(1 - \varepsilon)} \quad (3)$$

where μ = viscosity of the fluid. Richardson & Meikle (1961) plotted f as a function of the modified Reynolds number Re_1 to correlate sedimentation and fluidization data for spheres. To simplify calculations when V is not known *a priori*, Richardson & Meikle (1961) introduced a dimensionless group φ to be used instead of the friction factor f:

$$\varphi = fRe_1^2 = \frac{\varepsilon^3}{(1 - \varepsilon)^2} \frac{\psi^3 d_{eq}^3 \rho(\rho_p - \rho)g}{216\mu^2} \quad (4)$$

Establishing a quantitative relationship between φ and Re_1 allows the prediction of expanded bed porosity ε as a function of fluid properties (viscosity μ, density ρ), media properties (sphericity ψ, size d_{eq}, density ρ_p) and hydraulic loading rate ($V = Q/A$). Once the porosity (ε) is calculated, expanded bed height L can be computed using the relation $L(1 - \varepsilon) = L_0(1 - \varepsilon_0)$ with a knowledge of initial porosity ε_0 and initial bed height L_0. In certain problems, the desired expanded bed height L is given and the corresponding backwash velocity is to be calculated. In this case, the calculations proceed as follows. The porosity ε is first calculated from the expanded bed height L using the relation $L(1 - \varepsilon) = L_0(1 - \varepsilon_0)$, and this value of porosity is inserted into the definitions of Re_1 (Equation (3)) and φ

(Equation (4)). The relation between φ and Re_1 is then employed to calculate the velocity V. Depending on the relation (graphical or mathematical) between φ and Re_1, one or both of these two types of calculation may require trial-and-error solutions.

It has been noted that the Fair–Hatch fluidization Equation (Fair & Hatch 1933) and the Ergun Equation (Ergun 1952) – the latter when applied to fluidized beds – are actually correlations relating φ and Re_1 (Akgiray & Saatçi 2001):

$$\varphi = kRe_1 \quad (5)$$

$$\varphi = k_1 Re_1 + k_2 Re_1^2 \quad (6)$$

A number of authors have suggested the application of one or the other of these two equations to the fluidization of non-spherical media (Fair & Hatch 1933; Foust *et al.* 1960; Kelly & Spottiswood 1982; Geankoplis 1993; McCabe *et al.* 2001; Akgiray & Saatçi 2001). It seems plausible that these equations are applicable to both spherical and non-spherical media for the following reasons: (1) the definitions of Re_1 and φ include the sphericity parameter (cf Equations (3) and (4)), and therefore the particle shape appears to be accounted for in these equations and (2) the corresponding Equations (the Blake–Kozeny and Ergun equations) for fixed beds are generally accepted to be applicable to both spherical and non-spherical media. Recent research has shown, however, that when fluidized non-spherical media are considered, the value of the group φ is not uniquely fixed when Re_1 is fixed and the effect of shape has to be accounted for explicitly and independently. This is explained in what follows.

While Richardson & Meikle considered only spheres (i.e. the case $\psi = 1$), Dharmarajah & Cleasby (1986) considered the possibility of applying this method of correlation to non-spherical media. They have analyzed the data for fluidized spheres published by Wilhelm & Kwauk (1948) and Loeffler (1953) and the non-spherical particle data obtained by Cleasby & Fan (1981) and Dharmarajah (1982) to develop the following piecewise correlation:

For $Re_1 < 0.2 : \varphi = 3.01 Re_1$ \quad (7a)

For $Re_1 > 0.2$:

$$\log \varphi = 0.56543 + 1.09348 \log Re_1 + 0.17979 (\log Re_1)^2$$

$$- 0.00392 (\log Re_1)^4 - 1.5 (\log \psi)^2 \qquad (7b)$$

It is noteworthy that this piecewise correlation has been included in the last two editions of AWWA's *Water Quality Handbook* (AWWA 1990, 1999) and probably represents the "state-of-the-art" for the expansion of non-spherical media (Droste 1997).

An important experimental finding in the work by Dharmarajah & Cleasby (1986) was that, when φ versus Re_1 values were plotted, fluidization data for non-spherical media deviated from the trend-line of the spherical particle data. Akgiray *et al.* (2004) tested this finding using new data with silica sand and crushed glass. They verified that the non-spherical particle data do indeed deviate from the trend-line for spheres, but they also reported that the effect of shape is not well represented by the term $1.5(\log \psi)^2$ in Equation (7b).

A number of shortcomings of Equation (7a) and (7b) were also documented by Akgiray *et al.* (2004). More recently, Akgiray & Soyer (2006) presented a new equation to remedy these shortcomings. They have used the same spherical particle data utilized by Dharmarajah & Cleasby (1986) plus the spherical particle data by Wen & Yu (1966) and Hartman *et al.* (1989) to develop the coefficients in their equation:

$$\varphi = k_1 Re_1 + k_2 Re_1^P \qquad (8)$$

The following values were obtained: $k_1 = 3.137$, $k_2 = 0.673$ and $P = 1.766$ ($r^2 = 0.99897$, based on 600 data points). When attention is restricted to spheres, Equation (8) has a number of important advantages over Equation (7a) and (7b) (Akgiray & Soyer 2006).

As it stands, Equation (8) is applicable to spheres only. Based on the finding by Dharmarajah & Cleasby (1986) that the data ($\log \psi$ values) for non-spherical particles fall below the trend-line for spheres by a distance $1.5 (\log \psi)^2$, this term could be subtracted from the logarithm of the right-hand side of Equation (8) to obtain an equation applicable to non-spherical particles as well. However, Akgiray *et al.* (2004) reported new data using silica sand and crushed glass

and noted that the effect of shape was stronger than that predicted by the term $1.5 (\log \psi)^2$. Furthermore, the shape effect (as taken into account by such an additional term) was observed to depend on the modified Reynolds number. A new equation, however, was not presented in that paper to quantify the dependence of the shape effect on the Reynolds number and the sphericity. In addition to reporting a significant amount of additional experimental data, this paper presents an amendment of Equation (8) based on an analysis of the mentioned non-spherical particle data.

The current paper focuses on single-medium beds consisting of uniform (i.e. single size) grains. If an accurate model for the expansion of a uniform bed is available, the expansion of a non-uniform bed can also be predicted: A bed with a size gradation is considered to consist of several layers of approximately uniform size according to the sieve analysis data, and the expansion of each layer is separately calculated. The total expansion is calculated by adding the expansions of all the layers (Fair *et al.* 1971; AWWA 1999). This calculation method can also be used to predict the total expansion of a multimedia bed.

EXPERIMENTAL

In the first part of this work (Akgiray & Soyer 2006), fluidization experiments were carried out with glass balls of eight different sizes and plastic balls of three different sizes (Table 1). To assess the effect of particle shape, new experiments have been carried out with ten sieved fractions of silica sand, eleven sieved fractions of crushed glass, five sieved fractions of perlite and four sieved fractions of garnet sand (Table 2). Perlite and crushed glass are of interest as they are possible substitutes for silica sand in rapid filters (Uluatam 1991; Rutledge & Gagnon 2002). Their properties (densities and sphericities) are different than those of silica sand and, as such, they provide additional fluidization data useful for model development and testing. Data for four fractions of crushed glass were reported in earlier work (Akgiray *et al.* 2004). To obtain additional fractions of this material, crushed glass retained in the topmost sieve tray was crushed again and sieved. In this manner sufficient quantities of seven additional fractions of crushed glass

Table 1 │ Properties of the spherical media used in the fluidization experiments

Particle type	ρ_p (g/cm³)	d (mm)
Glass balls	2.519	1.11
Glass balls	2.494	1.19
Glass balls	2.529	2.03
Glass balls	2.494	3.18
Glass balls	2.532	2.99
Glass balls	2.499	4.03
Glass balls	2.529	4.98
Glass balls	2.527	6.01
Plastic balls	1.171	1.97
Plastic balls	1.193	2.48
Plastic balls	1.180	2.87

Table 2 │ Properties of the non-spherical media used in the fluidization experiments (crushed glass fractions marked (∗) were obtained by repeated crushing and sieving)

Particle type	Density ρ_p (g/cm³)	d_{eq} (mm)	Sphericity, ψ
Silica sand 0.355 × 0.50	2.646	0.50	0.710
Silica sand 0.50 × 0.59	2.647	0.60	0.777
Silica sand 0.50 × 0.60	2.649	0.65	0.794
Silica sand 0.59 × 0.60	2.651	0.68	0.788
Silica sand 0.59 × 0.70	2.653	0.73	0.772
Silica sand 0.70 × 0.84	2.640	0.84	0.757
Silica sand 0.84 × 1.00	2.639	1.02	0.738
Silica sand 1.00 × 1.19	2.641	1.11	0.706
Silica sand 1.19 × 1.41	2.628	1.40	0.714
Silica sand 1.41 × 1.68	2.629	1.65	0.723
Crushed glass 0.84 × 1.00	2.486	0.92	0.413
Crushed glass 1.18 × 1.41	2.494	1.24	0.442
Crushed glass 1.41 × 1.68	2.496	1.48	0.430
Crushed glass 2.00 × 2.38	2.499	2.08	0.415
Crushed glass 0.70 × 0.84 (∗)	2.490	0.77	0.530
Crushed glass 0.84 × 1.00 (∗)	2.497	0.98	0.516
Crushed glass 1.00 × 1.18 (∗)	2.497	1.13	0.548
Crushed glass 1.18 × 1.41 (∗)	2.496	1.34	0.515
Crushed glass 1.41 × 1.68 (∗)	2.503	1.62	0.564
Crushed glass 1.68 × 2.00 (∗)	2.501	1.82	0.559
Crushed glass 2.00 × 2.38 (∗)	2.499	2.21	0.624
Perlite 0.70 × 0.84	2.335	0.85	0.652
Perlite 0.84 × 1.00	2.331	1.07	0.645
Perlite 1.00 × 1.18	2.332	1.22	0.664
Perlite 1.18 × 1.41	2.328	1.41	0.651
Perlite 1.41 × 1.68	2.326	1.65	0.682
Garnet 0.21 × 0.25	4.393	0.245	0.845
Garnet 0.21 × 0.25	4.124	0.241	0.817
Garnet 0.177 × 0.21	4.420	0.220	0.856
Garnet 0.177 × 0.21	4.107	0.208	0.800

were obtained. Glass fractions obtained by repeated crushing and sieving were observed to have higher sphericity values. Using this procedure, several crushed glass fractions with approximately the same size and density but different sphericities were produced. This allowed the collection of additional fluidization data to investigate the effect of shape on expansion behavior.

The silica sand, perlite, garnet and crushed glass fractions were obtained by a rigorous manual sieving procedure followed by an additional 1 min of manual sieving such that the change in weight during the latter was less than 1% for each fraction. Densities were measured by a water-displacement technique. Equivalent diameters have been measured by counting and weighing 200 grains of each fraction. Diameters of the spheres were also measured with a micrometer and excellent agreement with the counting-weighing method was observed. Following earlier investigators (Cleasby & Fan 1981; Dharmarajah & Cleasby 1986; Akgiray *et al.* 2004), sphericity of each material was determined by measuring the fixed-bed head loss (h) for each fraction and using the Ergun Equation (Ergun 1952):

$$\frac{h}{L_0} = \frac{k_1\mu}{\rho g}\frac{(1-\varepsilon_0)^2}{\varepsilon_0^3}\left(\frac{6}{\psi d_{eq}}\right)^2 V + \frac{k_2}{g}\frac{(1-\varepsilon_0)}{\varepsilon_0^3}\left(\frac{6}{\psi d_{eq}}\right)V^2 \qquad (9)$$

This equation can be rearranged as a quadratic equation in sphericity ψ:

$$\left[\frac{h}{L_0}\right]\psi^2 - \left[\frac{k_2}{g}\frac{(1-\varepsilon_0)}{\varepsilon_0^3}\left(\frac{6}{d_{eq}}\right)V^2\right]\psi$$
$$- \left[\frac{k_1\mu}{\rho g}\frac{(1-\varepsilon_0)^2}{\varepsilon_0^3}\left(\frac{6}{d_{eq}}\right)^2 V\right] = 0 \qquad (10)$$

Once the quantities within the square brackets are measured, the sphericity is determined by using the well-known quadratic formula.

The sphericity values reported in Table 2 are the mean values for several measurements. Head loss measurements were carried out with extreme care to make sure that bed height (and porosity) did not change and that air bubbles did not accumulate within the bed during the experiments. Accumulation of small air bubbles, in particular, decreases porosity (volume fraction available for flow) and may completely invalidate head-loss measurements. For the eleven different sizes of glass and plastic balls, the calculated sphericities were always very close to 1.0. This finding, in addition to showing that the Ergun equation is very accurate for fixed beds of spheres for the range of Reynolds numbers used in this study, provided a check of the validity of head-loss measurements and sphericity determinations carried out in the current work. The properties of the media are summarized in Tables 1 and 2.

Fluidization experiments were carried out using tap water. Initial bed height L_0 was recorded before each fluidization experiment. Temperature, flow rate Q and bed expansion L were recorded during each experiment. Viscosity and density of water at different temperatures were obtained from the literature (Perry & Green 1984). In earlier work, a 40 cm high column with an internal diameter of 38 mm was employed (Akgiray et al. 2004). The new data presented here were obtained using a 152 cm high column with an internal diameter of 50.5 mm. The use of the larger column allowed collecting data at higher expansions and over a greater range of Reynolds numbers and porosities. Porosities were calculated from bed weight, bed height and density values.

Wall effects were estimated using an empirical formula based on Loeffler's data (Loeffler 1953) as explained in previous work (Akgiray & Soyer 2006). In this approach, the ratio of corrected velocity to actual velocity V_0/V is calculated from media properties and column diameter. Here V_0 is the backwash velocity required to attain the same porosity in an infinitely large container as velocity V would produce in a container of diameter D. The corrected velocity (V_0) values were used to plot and analyze the results. Although wall-effect corrections were always applied, it should be added that these corrections were quite small as the ratio V_0/V remained in the range 1.01–1.03 in all the experiments carried out in this work.

Experimental porosities were calculated from measured expansion heights using the relation $L(1 - \varepsilon) = L_0(1 - \varepsilon_0)$. The corrected velocities and calculated experimental porosities were then used together with fluid and particle properties to calculate Re_1 (Equation (3)) and φ (Equation (4)) values.

RESULTS AND DISCUSSION

Two sample sets of data are shown in Figures 1 and 2. Percent expansion versus backwash velocity is plotted in these figures:

$$\text{Percent expansion} = 100\frac{(L - L_0)}{L_0} \qquad (11)$$

Also shown (dashed line) are the percent expansions predicted using the Dharmarajah–Cleasby correlation (Equation (7a) and (7b)). The solid lines have been obtained with the new Equation (14) explained in the next section. These model lines were calculated as follows: values of fluid properties (μ, ρ), media properties (ψ, d_{eq}, ρ_p) and velocity (V) were inserted into the expressions for Re_1 (Equation (3)) and φ (Equation (4)). The corresponding theoretical porosity value was next calculated by inserting the expressions for Re_1 and φ into either Equation (7a) and (7b) or Equation (14) and then solving the resulting nonlinear algebraic equation for porosity by means of an iterative scheme. Once the theoretical porosity is determined, percent expansion is next calculated using Equation (11) and the relation $L(1 - \varepsilon) = L_0(1 - \varepsilon_0)$. Results similar
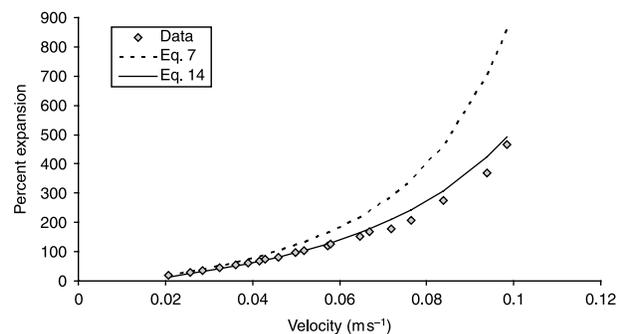

Figure 1 │ Bed expansion versus velocity for the 1.00 × 1.19 mm silica sand ($\psi = 0.706$).
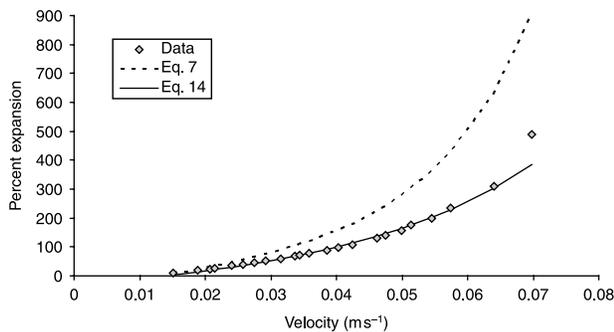
Figure 2 │ Bed expansion versus velocity for the 0.70 × 0.84 mm re-crushed glass ($\psi = 0.530$).

to Figures 1 and 2 were obtained for each of the materials in Table 2.

As noted earlier, the Dharmarajah–Cleasby correlation is considered to be the "state-of-the-art" for the prediction of filter bed expansion (Droste 1997; AWWA 1999). This correlation is mentioned and used in the discussion and evaluation of the results obtained here for the following reasons: (1) since it is widely used, its accuracy needs to be evaluated and this is accomplished presently; (2) it is used here as a basis of comparison because, to be useful, any new correlation should be simpler and/or more accurate than this correlation; (3) Equations (5) and (6) are no longer mentioned, as it has already been established that they are restricted to spheres and to limited ranges of Reynolds numbers and (4) other correlations proposed for non-spherical media require additional and difficult-to-obtain information such as settling velocities (Cleasby & Fan 1981). Prediction of settling velocities for non-spherical particles is notoriously unreliable (Kelly & Spottiswood 1982) and therefore additional tedious experiments would be required to obtain such information. Expansion correlations that require a knowledge of settling velocities have therefore been excluded from consideration in this work.

In evaluating the results of fluidization experiments, it is important to consider percent expansions (as in Figures 1 and 2), and not just porosities. This is because: (1) in many practical applications, percent expansion and expanded bed height are the quantities of direct interest and (2) errors in predicted values of bed height and percent expansion may be concealed when only porosities are considered. In Figure 1, for example, the measured porosity at the

rightmost point ($V = 0.1$ m/s) is 0.90, whereas Equation (7a) and (7b) predicts $\varepsilon = 0.94$. Percent error in porosity is then $100 \times (0.94 - 0.90)/0.90 = 4.3\%$, whereas the percent error in predicted percent expansion is $100 \times (857 - 466)/466 = 84\%$. Obviously, this error is unacceptably high. This issue is further discussed in earlier work (Akgiray & Soyer 2006).

Figures 3–7 display the non-spherical particle data collected in this work. The data for spheres were previously presented (Akgiray & Soyer 2006). The lines labeled "spheres" in Figures 3–7 were obtained using Equation (8) which represents the spherical particle data very accurately. The following are concluded: (1) while the Dharmarajah–Cleasby correlation (Equation (7a) and (7b)) is quite accurate for spheres, it consistently over-predicts the expansion of beds of non-spherical media and, in general, it is not accurate for such media: its deviation from the data increases as sphericity decreases; (2) when $\log \varphi$ versus $\log Re_1$ values are plotted, non-spherical particle data deviate from the trend-line of the spherical particle data. This deviation increases as sphericity decreases; (3) the observed deviation is larger than that predicted by the term $1.5 \, (\log \psi)^2$ and (4) careful examination of the data shows that the mentioned deviation depends on the Reynolds number as well.

THE NEW EQUATION

Equation (8) was developed in earlier work (Akgiray & Soyer 2006) using spherical particle data (600 separate measurements) from the literature and further tested using the data (332 measurements with the spheres listed
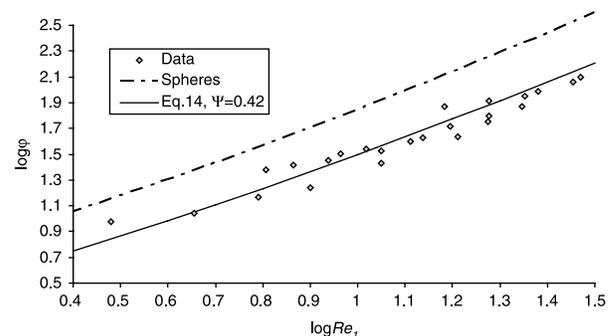

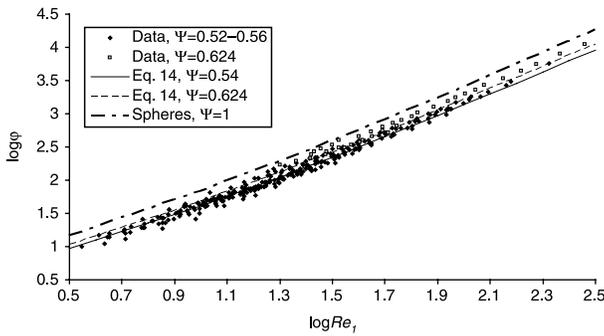**Figure 3** │ Data collected in this work for the four fractions of once-crushed glass.

Figure 4 │ Data for the seven re-crushed glass fractions (marked by (∗) in Table 2).

Figure 6 │ Data for the four fractions of garnet sand.

in Table 1) collected in the first phase of this work. For the range of Reynolds numbers and porosities spanned by the mentioned data $(-1.96 < \log Re_1 < 3.54$ and $0.37 < \varepsilon < 0.90)$, Equation (8) has been found to be more accurate than all of the existing popular correlations (for details, see Akgiray & Soyer (2006)). Based on the findings of previous work (Akgiray et al. 2004) and the large number of new measurements presented here, it is concluded that when $\log \varphi$ versus $\log Re_1$ values are plotted, the non-spherical particle data deviate from the trend-line of the spherical particle data, and the magnitude of this deviation depends on both the sphericity and the Reynolds number. The following equation form has therefore been adopted in this work:

$$\log\varphi = \log\left(3.137\,Re_1 + 0.673\,Re_1^{1.766}\right) + h(Re_1, \psi) \quad (12)$$

Here $h = h(Re_1, \psi)$ is a function of Re_1 and ψ, and it must satisfy the condition $h(Re_1, \psi = 1) = 0$. That is, the second term in Equation (12) vanishes for spheres. Note that
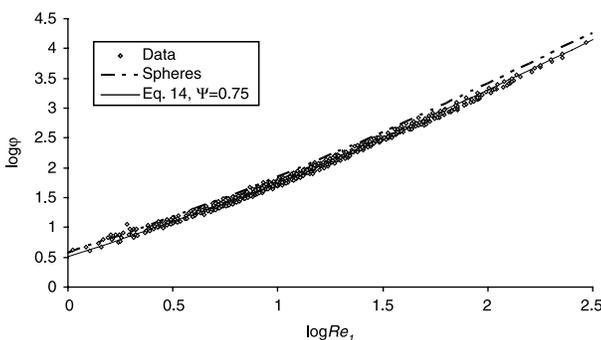
Equation (12) is developed by adding a term to Equation (8) and that it reverts to Equation (8) for spheres Numerous different expressions for h were tested and the following expression has been found to represent the data very accurately:

$$h(Re_1, \psi) = (a + b \log Re_1)(-\log \psi)^c \quad (13)$$

It should be emphasized that several different and more complicated expressions were also tested, but no significant improvement in accuracy over Equation (13) could be obtained by the use of more complex expressions and a larger number of adjustable coefficients. Equation (13) is arguably the simplest form conceivable for the function $h(Re_1, \psi)$, as it assumes a linear dependence on $\log Re_1$ and a simple proportionality to a power of $\log \psi$, while at the same time satisfying the condition $h(Re_1, 1) = 0$. A non-linear regression analysis has been carried out using the non-spherical particle data collected in this work to determine the best values of a, b and c. The following values are obtained: $a = -0.930$, $b = -0.274$ and $c = 1.262$

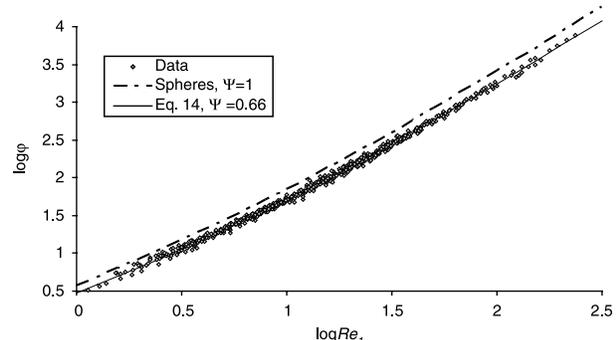**Figure 5** │ Data for the ten fractions of silica sand.

Figure 7 │ Data for the five fractions of perlite.

with $r^2 = 0.995$. Inserting these values, the following final equation is obtained, applicable to both spherical and non-spherical beds of particles:

$$\log \varphi = \log\left(3.137\,Re_1 + 0.673\,Re_1^{1.766}\right) - (0.930$$
$$+ 0.274 \log Re_1)(-\log \psi)^{1.262} \qquad (14)$$

The accuracy of this equation can be seen by inspecting Table 3 and Figures 8 and 9. Table 3 shows the mean error values obtained with Equations (7a), (7b) and (14). The mean error values for spheres are based on 332 measurements made in the first phase of this work plus 600 measurements collected from the literature (Akgiray & Soyer 2006). It is seen that the Dharmarajah–Cleasby correlation (Equation (7a) and (7b)) and the proposed Equation (14) are both very accurate for spheres. It should be noted, however, that Equation (14) is considerably simpler in form. For non-spherical materials, Equation (14) is again very accurate, whereas the use of the Dharmarajah–Cleasby correlation leads to rather large errors. When all the non-spherical particle data (1486 separate measurements) are considered together, the mean errors for Equation (7a) and (7b) and Equation (14) are 4.46% and 1.83%, respectively. The corresponding mean percent errors in predicted percent expansions are 39.0% (Equation (7a) and (7b)) and 13.7% (Equation (14)), respectively. The rows of Table 3 show that the Dharmarajah–Cleasby correlation deteriorates rapidly as sphericity decreases. Figure 8 displays experimental versus predicted porosity values. Percent expansion values are shown in Figure 9. These two figures are based on all the non-spherical particle
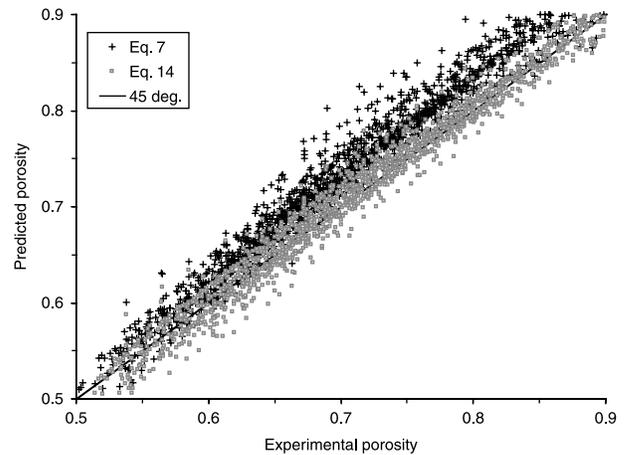

Figure 8 │ Experimental porosity versus predicted porosity for the non-spherical particle data collected in this work.

data collected in this work, i.e. 1486 measurements with the materials listed in Table 2. It is again observed that the proposed equation is considerably more accurate. The deviation of the Dharmarajah–Cleasby correlation from experimental data increases as porosity and percent expansion increase. The difference in the accuracies of the two correlations can be seen more clearly in Figure 9.

APPLICABILITY OF THE NEW EQUATION

Equation (14) is applicable to commonly used rapid filter media in the range of all backwash velocities that

Table 3 │ Percent errors in the predicted values of porosity for the data collected in this work

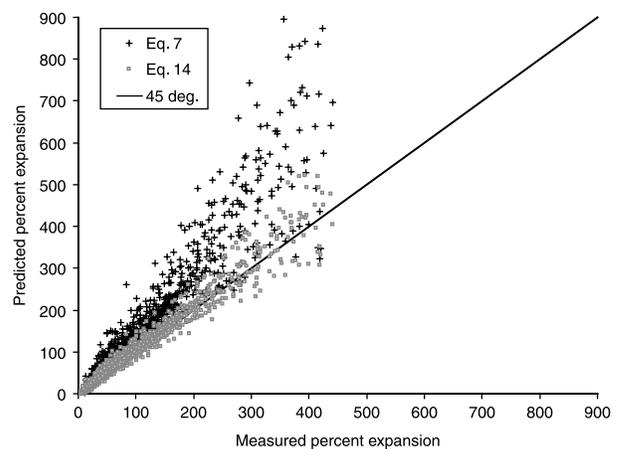| Material	Mean error with Equation (7a) and (7b)	Mean error with Equation (14)
Silica sand	3.74	1.96
Garnet	4.40	3.73
Perlite	4.09	1.20
Glass crushed once	9.21	3.99
All glass fractions	6.24	2.36
All non-spherical media	4.46	1.83
Spheres	2.35	2.26

Figure 9 │ Experimental percent expansion versus predicted expansion for the non-spherical particle data collected in this work.

may conceivably be employed in practice. The equation, however, is not limited to filter backwashing and it may be prudent here to discuss the limitations on its application in the context of liquid–solid fluidization in general. Non-spherical particle data used to develop and test this equation span the following parameter ranges: $0.40 < \varepsilon < 0.90, -0.76 < \log Re_1 < 2.51$ $(0.17 < Re_1 < 326), 0.40 < \psi < 1.0$. The limitations of Equation (14) can therefore be stated as follows. (i) Equation (14) should not be used for porosity values larger than about 0.90. This limitation is relevant for all correlations based on the fixed-bed friction factor concept, e.g. the Fair–Hatch equation, the Ergun equation and the Dharmarajah–Cleasby correlation (Akgiray & Saatçi 2001). As a matter of fact, it is generally accepted that expansion behavior of fluidized beds change at about $\varepsilon = 0.85$–0.90 and—whatever the method of correlation used is—a different equation is usually specified for higher expansions (Dharmarajah & Cleasby 1986; Di Felice 1995). (ii) Equation (14) is based on Equation (8) which, in turn, was developed and tested using data in the range $-1.96 < \log Re_1 < 3.54$, whereas the non-spherical particle data used in this work span the range $-0.76 < \log Re_1 < 2.51$. The accuracy of Equation (14) outside these ranges of Reynolds numbers has not been evaluated. (iii) The shape correction term is based on data with $\psi > 0.4$: Extreme shapes, such as needles, and flat objects, such as flakes, have not been studied. For most practical applications, these limitations will not prevent the use of Equation (14). Porosities remain well below 0.90, for example, during filter backwashing. Similarly, during backwashing rapid filter media, it can be shown that Reynolds numbers are well inside the stated range. Furthermore, the sphericities of all the commonly used rapid filter media are reported to be above about 0.45 (AWWA 1999). (iv) It is also possible to insert $\varepsilon = \varepsilon_{mf}$ in Equation (14) to get an estimate of the minimum fluidization velocity V_{mf}. Epstein (2003a) noted that, because expansion equations are usually correlations based on a whole range of porosity values (from ε_{mf} to very high ε values), they are likely to be less accurate at the ε_{mf} extremity than an equation which is tailored to this extremity. It is therefore recommended that Equation (14) is applied at bed expansions above about 10% and a specialized equation be used if the value of V_{mf} is desired.

SUMMARY AND CONCLUSIONS

Fluidization experiments have been carried out with glass balls, plastic balls and carefully sieved fractions of silica sand, garnet sand, perlite and crushed glass to ascertain the effect of shape on expansion behavior. Sphericity of each material was determined using fixed-bed head loss data in conjunction with the Ergun equation. For all the materials studied, sphericity values calculated using fixed-bed head loss measurements and the Ergun equation allowed successful prediction of the effect of particle shape on bed expansion during fluidization. The non-spherical particle data fall below the curve for spheres on the friction factor versus the modified Reynolds number diagram. A new equation is developed using the non-spherical particle data collected in this work. The equation has the following advantages: (1) it has been found to be very accurate for all the materials tested; (2) it does not require a knowledge of terminal settling velocities of the media grains; (3) it has a simple form and (4) it can be applied to both spherical and non-spherical media. In addition to the spherical particle data involving 600 bed expansion measurements compiled from the literature, the proposed equation has been developed and tested by using a substantial amount of bed expansion measurements (332 measurements with spheres and 1486 separate measurements with beds of non-spherical particles) carried out during this work.

REFERENCES

Akgiray, O. & Saatçi, A. M. 2001 A new look at filter backwash hydraulics. *Water Sci. Technol.: Water Supply* **1**(2), 65–72.

Akgiray, O. & Soyer, E. 2006 An evaluation of expansion equations for fluidized solid-liquid systems. *J. Water Supply Res. Technol. Aqua* **55**(7–8), 517–526.

Akgiray, O., Soyer, E. & Yuksel, E. 2004 Prediction of filter expansion during backwashing. *Water Sci. Technol.: Water Supply* **4**(5–6), 131–138.

Akkoyunlu, A. 2003 Expansion of granular water filters during backwash. *Environ. Eng. Sci.* **20**(6), 655–665.

AWWA 1990 *Water Quality and Treatment, A Handbook of Community Water Supplies*, 4th edition. McGraw-Hill, New York.

AWWA 1999 *Water Quality and Treatment, A Handbook of Community Water Supplies*, 5th edition. McGraw-Hill, New York, ch 8.

Blake, C. F. 1922 The resistance of packing to fluid flow. *Trans. Am. Inst. Chem. Eng.* **14**, 415.

Cleasby, J. L. & Fan, K. 1981 Predicting fluidization and expansion of filter media. *J. Environ. Eng. Div. ASCE* **107**(EE3), 455–471.

Couderc, J. P. 1985 Incipient fluidization and particulate systems. In: Davidson, J. F., Clift, R. & Harrison, D. (eds) *Fluidization*. Academic Press, New York, pp. 1–46.

Dharmarajah, A. H. 1982 *Effect of Particle Shape on Prediction of Velocity-Voidage Relationship in Fluidized Solid-Liquid Systems*. Doctoral dissertation, Iowa State Univiversity, Ames, IA.

Dharmarajah, A. H. & Cleasby, J. L. 1986 Predicting the expansion behavior of filter media. *J. AWWA* **78**(12), 66–76.

Di Felice, R. 1995 Hydrodynamics of liquid fluidization. *Chem. Eng. Sci.* **50**(8), 1213–1245.

Droste, R. L. 1997 *Theory and Practice of Water and Wastewater Treatment*. John Wiley & Sons, New York, ch 14.

Epstein, N. 2003a Liquid–solid fluidization. In: Yang, W. C. (ed.) *Handbook of Fluidization and Fluid-Particle Systems*. Marcel Dekker, New York, pp. 705–764.

Epstein, N. 2003b Applications of liquid–solid fluidization. *Int. J. Chem. Reactor Eng.* **1**, 1–16.

Ergun, S. 1952 Fluid flow through packed columns. *Chem. Eng. Prog.* **48**(2), 89–94.

Fair, G. M., Geyer, J. C. & Okun, D. A. 1971 *Elements of Water Supply and Wastewater Disposal*, 2nd edition. John Wiley and Sons, New York.

Fair, G. M. & Hatch, L. P. 1933 Fundamental factors governing the stream-line flow of water through sand. *J. AWWA* **25**(11), 1551.

Foust, A. S., Wenzel, L. A., Clump, C. W., Maus, L. & Andersen, L. B. 1960 *Principles of Unit Operations corrected 2nd printing*. Wiley International Edition, Japan.

Garside, J. & Al-Dibouni, M. R. 1977 Velocity-voidage relationships for fluidization and sedimentation in solid-liquid systems. *Ind. Eng. Chem. Process. Des. Dev.* **16**(2), 206–214.

Geankoplis, C. J. 1993 *Transport Processes and Unit Operations*, 3rd edition. Prentice-Hall International, London.

Hartman, M., Havlin, V., Svoboda, K. & Kozan, A. P. 1989 Predicting voidage for particulate fluidization of spheres by liquids. *Chem. Eng. Sci.* **44**(11), 2770–2775.

Kelly, E. G. & Spottiswood, D. J. 1982 *Introduction to Mineral Processing*. John Wiley & Sons, New York, pp. 77–78.

Loeffler, A. L. Jr. 1953 *Mechanisms of Hindered Settling and Fluidization*. Doctoral dissertation, Iowa State University of Science and Technology, Ames, IA.

McCabe, W. L., Smith, J. C. & Harriot, P. 2001 *Unit Operations of Chemical Engineering*, 6th edition. McGraw-Hill, New York, pp. 176–178.

Perry, R. H. & Green, D. 1984 *Perry's Chemical Engineers' Handbook*, 6th edition. McGraw-Hill, New York.

Richardson, J. F. & Meikle, R. A. 1961 Sedimentation and fluidization part III. *Trans. Inst. Chem. Eng.* **39**, 348–356.

Rutledge, S. O. & Gagnon, G. A. 2002 Assessment of crushed-recycled glass as filter media for small-scale water treatment applications. *J. Environ. Eng. Sci.* **1**(5), 349–358.

Uluatam, S. S. 1991 Assessing perlite as a sand substitute in filtration. *J. AWWA* **83**(6), 70–71.

Wen, C. Y. & Yu, Y. H. 1966 Mechanics of fluidization *Chem. Eng. Prog. Symp. Ser.* **62**, AIChE, New York.

Wilhelm, R. H. & Kwauk, M. 1948 Fluidization of solid particles. *Chem. Eng. Prog.* **44**(3), 201–218.